ARTICLE

Electrochemical Control of Stability and Restructuring Dynamics in Au—Ag—Au and Au—Cu—Au Bimetallic Atom-Scale Junctions

Ping Shi and Paul W. Bohn*

Department of Chemical and Biomolecular Engineering and Department of Chemistry and Biochemistry, University of Notre Dame, Notre Dame, Indiana 46556

ABSTRACT Metallic atom-scale junctions (ASJs) are interesting fundamentally because they support ballistic transport, characterized by conduction quantized in units of $G_0 = 2e^2/h$. They are also of potential practical interest since ASJ conductance is extraordinarily sensitive to molecular adsorption. Monometallic Au ASJs were previously fabricated electrochemically using an I^-/I_3^- medium and a unique open working electrode configuration to produce slow electrodeposition or electrodissolution, resulting in reproducible ASJs with limiting conductance $<5\ G_0$. Here, bimetallic Au—Cu—Au and Au—Ag—Au ASJ structures are obtained by electrochemical deposition/dissolution of Cu and Ag in K_2SO_4 supporting electrolyte. The ASJs are fabricated in Si_3N_4-protected Au nanogaps obtained by focused ion beam milling, a protocol which yields repeatable and reproducible Au—Cu—Au or Au—Ag—Au ASJs without damaging the Au nanogap substrates. While Au—Ag—Au ASJs are relatively stable (hours) at open circuit potential in the supporting electrolyte, Au—Cu—Au ASJs exhibit spontaneous restructuring dynamics, characterized by monotonic, stepwise decreases in conductance under the same conditions. However, the Au—Cu—Au ASJs can be stabilized by applying sufficiently negative potentials. Hydrogen adsorption and shifts in the Fermi level are possible reasons for the enhanced stability of Au—Cu—Au structures at large negative overpotentials. In light of these observations, it is possible to integrate ASJs in microfluidic devices as renewable, nanostructured sensing elements for chemical detection.

KEYWORDS: nanowire · atom-scale junction · conductance quantization · electrochemical nanofabrication · nanocontact

Nanoscale materials often show properties and behavior different from those found in the corresponding bulk form, which can lead to novel applications. Among nanomaterials, metallic point contacts or atom-scale junctions (ASJs) are of fundamental and practical importance and have received extensive attention in recent years.[1−16] Not only are they the limiting case of small nanostructures and, as such, may constitute fundamental building blocks in future molecular electronic devices, but they also exhibit interesting properties which may lead to intriguing applications, such as single-atom transistors,[15] atomic switches,[17,18] and chemical sensors.[19,20] For example, ASJs exhibit ballistic transport of charge carriers, and their conductance is extraordinarily sensitive to molecular adsorption, making them excellent candidates for highly sensitive chemical sensors.[20−24] Given that these junctions are inherently atomic in size, it is not surprising that they exhibit interesting quantum phenomena, even at room temperature. The conductance is quantized by

$$G = (2e^2/h)\sum_{i=1}^{n} T_i \qquad (1)$$

where e is the electron charge, h is Planck's constant, and T_i is the transmission probability of the ith conduction channel (quantum mode).[3,25,26] For an ideal metal, such as gold, $T_i \approx 1$ for all channels. Hence, the conductance is quantized in the form of $G = nG_0$, where $G_0 = 2e^2/h$ (=1/12.9 kΩ) is the conductance quantum and the number of quantum modes, n, is dependent on the size of the ASJ.

ASJs can be fabricated either by mechanical means, for example, using scanning tunneling microscopy (STM) tips[1,2] or mechanically controllable break junctions (MCBJ),[4,27] or by electrochemical methods.[24,28−34] Although mechanical methods offer certain advantages, allowing for reliable and reproducible fabrication of ASJs with high yield and controllability, they usually require sophisticated positioning (*e.g.*, piezoelectric) devices, rendering them less attractive for chemical sensing applications. In contrast, electrochemical methods are economical and compatible with standard silicon microfabrication techniques and are, therefore, preferable for many practical applications. However, attaining precise control over the geometry of the ASJ is a challenge in electrochemical nanofabrication. Recently, a new electrodeposition/dissolution strategy was developed in

*Address correspondence to pbohn@nd.edu.

Received for review February 23, 2010 and accepted April 9, 2010.

Published online April 15, 2010. 10.1021/nn1003716

our laboratory, in which the working electrode (WE), that is, the nanogap substrate in these structures, is kept open during the electrochemical process, resulting in extremely slow charge transfer, which yields enhanced control over the stop-point in the process. In the open-WE protocol, the WE (or both working electrodes in the case of a nanogap) is not specifically wired into the potentiostat circuit, while the counter electrode is referenced to earth ground. The open-WE strategy has been successfully used to fabricate stable Au ASJs on silicon by either depositing Au in prefabricated Au nanogaps or electrochemically thinning overgrown Au junctions.[34] The significantly slowed electrode kinetics in the open-WE configuration are important because strategies to produce the smallest ASJs rely on monitoring the conductance through the junction and stopping the fabrication chemistry when a sufficiently small ASJ is reached, ideally at a conductance of $G = G_0$. Slow, controllable electrode kinetics, therefore, enhance the ability to fabricate extremely small ASJs. Unfortunately, repeated fabrication of Au ASJs, especially through electrodissolution of overgrown junctions, results in irreparable damage to the Au nanogaps, thus making formation of new ASJs much more difficult. Since the ultimate goal is to integrate ASJs into microfluidic and nanofluidic architectures as renewable chemical sensing elements, regenerabilty of ASJs is an important concern. In the present work, the open-WE electrochemical configuration was employed to fabricate ASJs incorporating a second metal, such as Cu or Ag, in the Au nanogaps. This strategy produces Au−Ag−Au and Au−Cu−Au bimetallic ASJs with significantly enhanced repeatability. Indeed, repetitive fabrication of Au−Ag−Au ASJs without significant damage to the Au nanogap substrates is feasible on the open silicon surface, and even in microfluidic channels, without further processing. Au−Cu−Au ASJs, on the other hand, exhibit spontaneous restructuring dynamics, characterized by monotonic changes in the conductance, in electrolyte solution at 300 K. However, the Au−Cu−Au ASJs can be stabilized by applying appropriate negative potentials to the WE.

RESULTS AND DISCUSSION

Recently, a unique open-WE electrochemical protocol was developed in our laboratory to fabricate monometallic ASJs. The experimental configuration is shown in Figure 1a, where a DC potential, E_{DC}, set by a potentiostat is applied to a Au wire, which serves as both the counter electrode (CE) and quasi-reference electrode (QRE). The working electrode itself (*i.e.*, the gold nanogap sample) is kept open during the electrochemical fabrication process. ASJ fabrication is terminated when the CE/QRE is removed from the solution or disconnected from the potentiostat (see the Experimental Section or ref 34 for details). In this mode of operation, the electrode kinetics are greatly slowed and controllability is enhanced, allowing ready fabrication of ASJs.[34] Stable Au ASJs were fabricated by combining open-WE with an I^-/I_3^- medium. The Au ASJs can, in favorable cases, exhibit relatively long lifetimes (>1 h). However, the iodide solution slowly oxidizes, yielding a solution that is a strong Au etchant which damages the ASJ as well as the Au nanogap substrate. Iodide-free media, such as perchloric acid, containing $HAuCl_4$ as the Au source, can also be used to fabricate Au ASJs electrochemically in the open-WE configuration. Although ASJs may be readily grown by electrodeposition starting from an FIB-milled nanogap in the $HClO_4/HAuCl_4$ medium, re-thinning the overgrown junctions back to atomic size is difficult because electrodissolution is not site-selective, and the Au nanogap substrate can be severely damaged before the desired re-thinning of the overgrown junction occurs. Figure 2 shows a scanning electron microscope (SEM) image of a sample after electrodissolution. A positive bias was applied (>1 h)

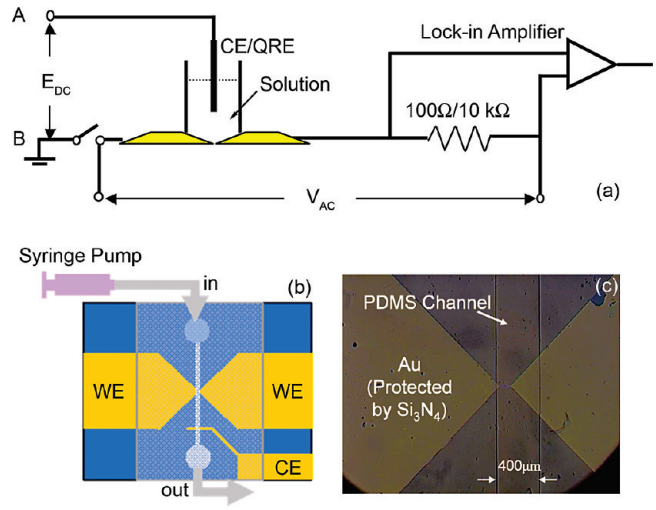

Figure 1. (a) Experimental configuration for electrochemical fabrication of atom-scale junctions. E_{DC} is set by the potentiostat and is equal to E(B) − E(A). The yellow regions represent the two sides of the nanogaps across which the ASJ is formed. (b) Schematic diagram of the sample used for fabrication of ASJs in microfluidic channels. (c) Photomicrograph of the center area of a bowtie-shaped Au film sample in a PDMS microfluidic channel. The width of the Au microbridge at the center of the tie is too small to be seen at this magnification.

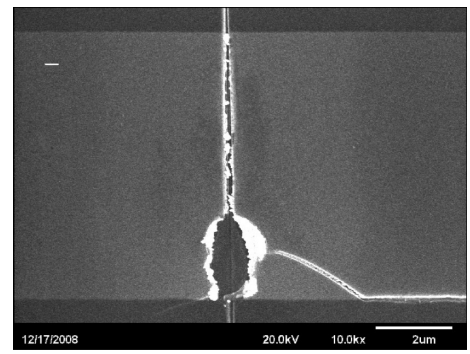

Figure 2. SEM image of an overgrown Au junction after electrodissolution. Damage to the structure is clearly evident near the bottom of the nanogap.

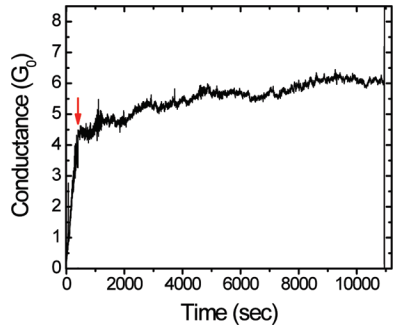

Figure 3. Conductance *vs* time trace of a Au−Ag−Au bimetallic ASJ fabricated by open-WE deposition (E_{DC} = −0.94 *vs* Au). The red arrow marks the time when the CE was emersed from the electrolyte solution.

to the overgrown Au junction in the electroplating medium (0.05 M $HClO_4$ containing 1 mM $HAuCl_4$) in order to thin the overgrown structure back to ASJ dimensions. As is clearly evident, a large Au gap formed under the protective SiN_x layer in the lower part of the nanogaps, but the junction still exhibited bulk-like conductance characteristic of overgrown Au in the upper part of the nanogap.

One simple approach to circumvent this problem is to fabricate bimetallic ASJs of the form A−B−A, where metal A (substrate) is chosen to be inert at the potential applied to thin (dissolve) metal B (ASJ). Cu and Ag are attractive candidates for metal B because their position in the electromotive series indicates that they are easier to oxidize than Au, and they possess an electronic configuration ($d^{10}s^1$) similar to Au and thus may be expected to exhibit comparable conductance quantization behavior. Thus, Ag and Cu were chosen as metal B to construct reproducible bimetallic A−B−A ASJs in FIB-milled Au nanogaps.

Au−Ag−Au Bimetallic ASJs. Figure 3 shows a typical conductance−time trace during the formation of a Au−Ag−Au ASJ in a Au nanogap by open-WE electrodeposition. Similar to the behavior shown by monometallic Au ASJs,[34] the growth rate of Ag is sufficiently slow at the negative bias used (E_{DC} = −0.94 V *vs* Au QRE) that the reaction can be terminated manually by disconnecting or removing the CE (a Au wire) from the solution. Once the CE is removed, the conductance of the Ag ASJ remains stable in the range of 5−6 G_0, indicating that electrodeposition is indeed well-terminated. The Ag ASJs fabricated by this open-WE display remarkable stability, lasting a few hours in favorable cases, long enough for chemical sensing applications.

Figure 4 shows the conductance associated with formation of a similar Au−Ag−Au bimetallic ASJ by the converse process of open-WE electrodissolution of an overgrown Ag junction. The electrodissolution is performed in three stages of roughly equal duration. From t = 0 to ~40 s, the CE is in solution and held near E_{DC} ~ −0.4 V, and conductance decreases near the end of the period. Then the CE is emersed from t = 40 s to ~70 s, resulting

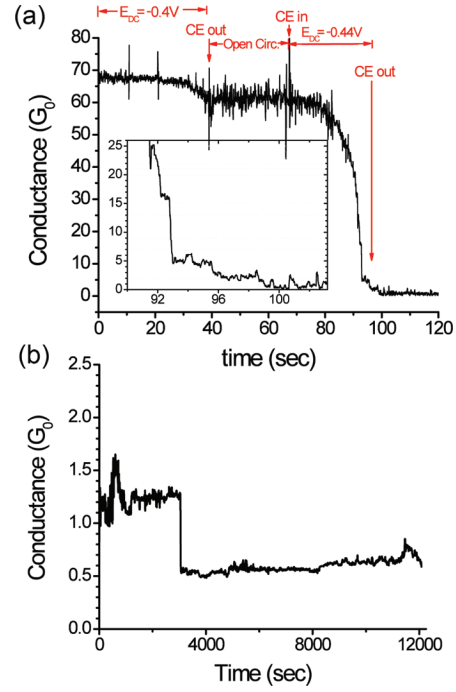

Figure 4. (a) Conductance *vs* time trace of a Au−Ag−Au bimetallic ASJ fabricated by open-WE electrodissolution of an initially overgrown Au−Ag−Au junction. (Inset) Expanded view of the region near the emersion of the CE. Data here were acquired with 100 Ω load resistance. (b) Long-term (t > 3 h) conductance of the Au−Ag−Au ASJ fabricated in panel (a). Data in this panel were acquired with 10 kΩ load resistance. Note the scales of both ordinate and abscissa in this panel.

in an open circuit, with little change in conductance. Finally, at t > 70 s, the CE is brought back into contact with the solution, and conductance decreases again, dramatically after ~90 s. In the latter time window, the electrodissolution proceeds through characteristic step-changes in conductance, exhibiting metastable conductance values near 25, 16, 5, and 3 G_0.

It is evident from this figure that, when the CE (Au wire) is in the solution with E_{DC} applied (but WE open), electrodissolution proceeds, but when the CE is removed from solution (*i.e.*, open circuit), electrodissolution ceases. Clearly, the controllability provided by this open-WE configuration is excellent, making it possible, in principle, to fabricate bimetallic ASJs of any size, as long as the ASJs are stable in solution, and this experiment generated a Au−Ag−Au bimetallic ASJ with a limiting conductance value close to 1 G_0. Figure 4b shows the long-term (t > 3 h) behavior of this ASJ conductance, using a load resistance, R_{ext} = 10 kΩ, which gives more accurate measurements for low conductance values. The figure shows that the conductance of this ASJ is stable at ~1.2 G_0 for *ca.* 1 h, at which point the conductance changes abruptly to ~0.5 G_0 and is stable at that value for *ca.* 3 h. The appearance of a stable, fractional conductance state at G ~ 0.5 G_0 is consistent with observations made in this laboratory and others and can potentially be ascribed to molecular ad-

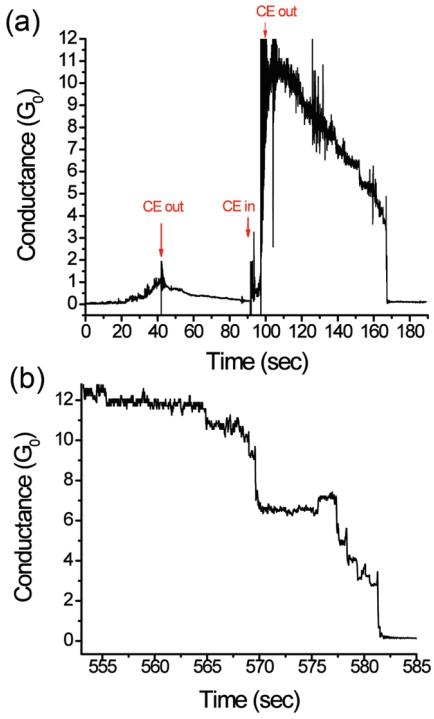

Figure 5. (a) Conductance *vs* time of a bimetallic Au−Cu−Au ASJ fabricated by open-WE deposition (E_{DC} = −1.2 V *vs* Au). (b) Expanded view of conductance variation during spontaneous restructuring of a regrown Au−Cu−Au ASJ (different sample than panel (a)).

sorption or spontaneous restructuring, although the abruptness of the transition appears inconsistent with molecular adsorption. A more detailed discussion of fractional conductance states is given below.

Au−Cu−Au Bimetallic ASJs. Fundamentally different behavior is observed for Au−Cu−Au ASJs. Figure 5 shows a typical conductance−time trace during the open-WE electrodeposition of a Au−Cu−Au ASJ on silicon at an applied potential E_{DC} = −1.2 V *vs* Au QRE. As is evident from the figure, Au−Cu−Au ASJs can also be easily fabricated with good controllability using open-WE electrodeposition. However, in contrast to the Au−Ag−Au bimetallic structures as well as Au monometallic ASJs, Au−Cu−Au ASJs are not stable at open circuit. Once the fabrication is terminated by emersing the CE, the conductance of the ASJ spontaneously decreases, leading eventually to a zero conductance state (*i.e.*, a broken wire). The spontaneous restructuring of Au−Cu−Au ASJs evident in Figure 5 occurs through quantized conductance states, as is clearly discernible in Figure 5b. After the Au−Cu−Au ASJs break, they can be repeatedly regenerated by electrodeposition, but the ASJs produced undergo spontaneous restructuring every time, showing stepwise variation of conductance during the thinning process in most cases. It normally takes ~30−60 s for a 10 G_0 junction to break spontaneously; however, after several reformation cycles, the process may take 3−4 min, an observation which is attributed to improved crystallinity of the structures, an effect of so-called electrochemical annealing.[30,31,35]

These results indicate that the Au−Cu−Au ASJs are intrinsically unstable at open circuit in the $CuSO_4/K_2SO_4$ electrolyte, consistent with the observation by other groups that monometallic Cu ASJs also have relatively short lifetimes under electrochemical conditions.[30,31,36]

Considering that Cu and Ag are both coinage metals with the same $d^{10}s^1$ electron configuration, one may ask why Au−Ag−Au bimetallic ASJs are stable at open circuit while Au−Cu−Au ASJs are not. First, consider the cohesive energy which is related to the strength of metallic bonds. The value for bulk Cu is 336 kJ/mol, which is larger than that for bulk Ag, 284 kJ/mol,[37] consistent with the fact that bulk Cu has a higher melting point (1360 K) than bulk Ag (1265 K).[38] Apparently, differences in bulk cohesive energy cannot explain the differing stabilities of Au−Ag−Au and Au−Cu−Au ASJs. However, on the nanoscale, the story may be different since it is known theoretically that cohesive energy decreases with size in nanoparticles.[37,39] Unfortunately, detailed measurements of the cohesive energy for atomic-sized Cu and Ag nanoparticles are not available. An alternative explanation focuses on the relationship between the reactivity of metals and the filling of d orbitals, which explains why bulk noble metals (Au, Ag, Cu) are relatively unreactive compared to transition metals, since they have filled d bands. However, at the nanoscale, the d bands of noble metals shift toward the Fermi level, making them more active than the corresponding bulk forms. Quantum chemical calculations show that the shift for Ag is relatively small, so the d bands are still far away from Fermi level, while for Cu, the shift is much larger and the d bands reach just below the Fermi level, making Cu similar in activity to transition metals at the nanoscale.[40,41] This observed change in electronic structure is certainly consistent with the ordering of stability observed between Au−Ag−Au and Au−Cu−Au ASJs and likely plays some role in determining the relative stabilities of Cu- and Ag-containing ASJs, although contributions from differences in cohesive energies of Ag and Cu nanoparticles cannot be ruled out.

Electrochemical Stabilization of Au−Cu−Au ASJs. One of the advantages of electrochemical methods for nanofabrication is that the electrical potential may be varied to induce changes in properties of the electrified interface, such as the electron density, surface stress, and work function. Thus, the interaction between the electrode and its environment makes it possible to fabricate stable metal nanostructures which may not be accessible by other methods.[42,43] Indeed, despite being unstable at open circuit, Au−Cu−Au bimetallic ASJs can be stabilized by applying an appropriate negative bias through the CE/QRE. Figure 6a shows the conductance *versus* time over the entire course of a cycle of growth, thinning and regrowth, finally terminated by an open circuit period that results in breaking the Au−Cu−Au ASJ. The results shown in this figure indicate that a −1.4

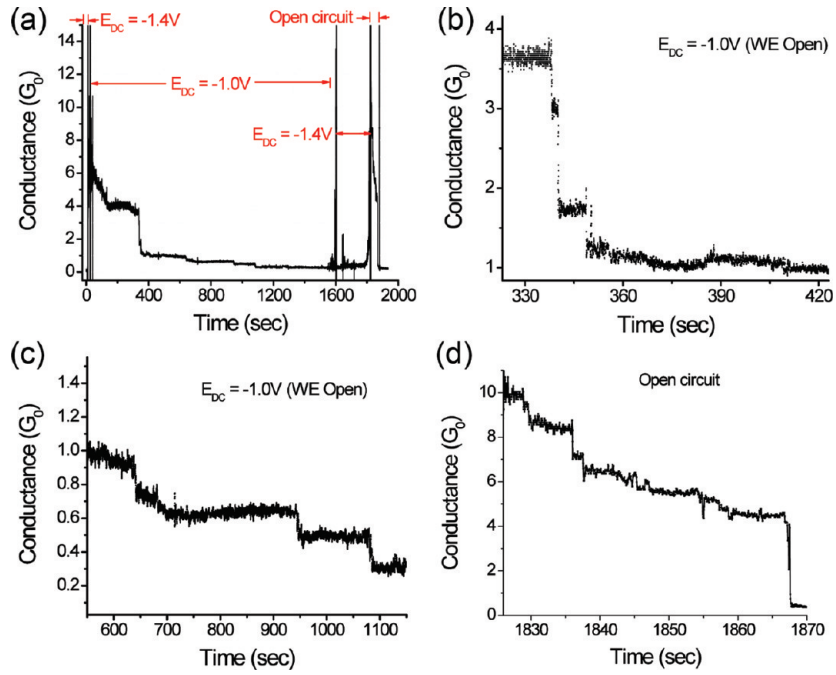

Figure 6. Conductance *vs* time for a Au−Cu−Au bimetallic ASJ under different bias conditions, showing restructuring dynamics and stability phenomena. (a) Entire course of the data collection with applied potentials, E_{DC}, in the indicated time intervals. (b−d) Expanded views during periods with different applied potentials, showing (b) approach to 1 G_0 at $E_{DC} = -1.0$ V; (c) fractional conductance behavior; and (d) thinning to the break point at open circuit.

V potential is sufficiently negative to form a Au−Cu−Au ASJ, but −1.0 V is not. Instead, at −1.0 V, the ASJ exhibits thinning but with much slower restructuring dynamics compared to open circuit potential, as is clearly illustrated in Figure 6b−d. In the period from t = 330 to 350 s, the conductance decreases in steps, approaching a metastable value of $G = 1\ G_0$, where it remains until $t \sim 650$ s, at which point it undergoes another series of stepwise decreases in conductance to various fractional conductance values, just as was observed in Figure 4 for the Au−Ag−Au ASJ.

Empirically, it is possible to find a negative potential to stabilize the Au−Cu−Au ASJs, and we hypothesize that under these conditions deposition and dissolution of Cu reach a quasi-steady state. Rather than remaining at $G = 1\ G_0$, the conductance continues to decrease to fractional values. Similar fractional conductance was first reported for Au ASJs under electrochemical conditions by Tao *et al.*[42−44] and later for other metallic ASJs by other groups in both electrochemical[31,45−48] and ultrahigh vacuum (UHV) environments.[49,50] The origin of fractional conductance in metallic nanowires is an interesting, but complicated, issue, and a consensus about its physical origin has not yet been reached. Possible explanations that have been put forth invoke the scattering of conduction electrons in monatomic junctions by adsorbed molecules or ions and/or structural deformation of the junction itself. For example, quantum calculations suggest a monatomic Au junction with equal spacing would exhibit $G = 1\ G_0$ while dimerized Au wire may yield a conductance of 0.4−0.6 G_0.[51] In addition, wires incorporating H_2 also show conductance smaller than 1 G_0 in theory.[52,53] Independent of the ultimate explanation, the Au−Cu−Au ASJ exhibiting fractional conductance remains competent to support regrowth of a high conductance ASJ, as indicated by the second application of $E_{DC} = -1.4$ V at ∼1600 s in Figure 6a.

The fact that sufficiently negative potentials stabilize Au−Cu−Au ASJs is also illustrated by the conductance histograms obtained under different bias conditions, *viz.* Figure 7. The conductance histogram at open circuit (Figure 7a) shows significant amplitude out to ∼5 G_0, consistent with the approximately constant rate of restructuring observed qualitatively in the data of Figures 5 and 6. However, under negative bias, small G values dominate, as seen in Figure 7b. We advance two possible reasons for the electrochemical stabilization of Au−Cu−Au ASJs: hydrogen adsorption, or even incorporation, and potential-induced shifts in the Fermi level. Despite the fact that hydrogen does not adsorb on bulk Cu, nanostructured Cu may have a much greater affinity to hydrogen because the d bands are located just below the Fermi level,[40] as discussed earlier. Indeed, Tao *et al.*[22] and later Kiguchi *et al.*[45,47,54] found that Au and Cu atomic-scale contacts fabricated by STM and MCBJ exhibit stronger mechanical properties at the hydrogen evolution potential than in the double-layer region, an observation that could be explained by a decrease in surface energy caused by hydrogen adsorption on the metal nanocontacts.[46] Similar stabilization of atom-sized contacts under negative potential was also observed by Li *et al.* for monatomic contacts of Pd, a metal which is well-known to have great affin-

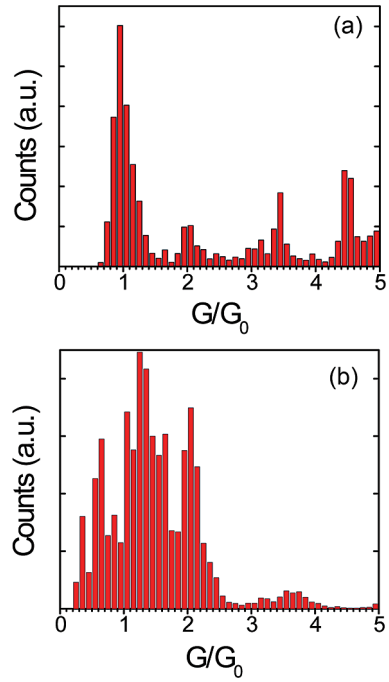

Figure 7. Conductance histograms of Au−Cu−Au bimetallic ASJs under (a) open circuit; and (b) $E_{DC} = -1.1$ V (WE open).

ity to hydrogen, indicating that hydrogen adsorption may play an important role in electrochemical stabilization.[48] The stabilization of metal nanowires by adsorption of hydrogen and other molecules has also been reported for Au,[49,55] Pd,[56] Pt,[57] Cu,[58] Ag,[55] and Ni[59,60] as well as Al, Ta, and Nb.[61] Another reason for electrochemical stabilization could simply be thermodynamics. When sufficiently negative potentials are applied (negative compared to the potential of zero charge of the electrode), the Fermi level of the electrode increases, increasing the overpotential for electrodeposition, making the Au−Cu−Au ASJs more difficult to dissolve.

As demonstrated above, both Au−Ag−Au and Au−Cu−Au bimetallic ASJs can be successfully fabricated using the open-WE electrochemical nanofabrication protocol with good controllability. The same approach can also be employed to fabricate ASJs in microfluidic channels. In this case, since the CE is patterned directly on the substrate surface (Figure 1b), the CE is simply disconnected to terminate the electrochemical process because it cannot be physically removed. The open-WE approach to forming bimetallic ASJs in Au nanogaps has been successfully used to fabricate Au−Ag−Au and Au−Cu−Au ASJs in PDMS microfluidic channels. Once formed, the structures can be removed either by electrodissolution or by chemical treatment, and the resulting structures are found to be competent for many repetitive growth cycles without damaging the Au substrate. Even heavily overgrown samples can be treated in H_2O_2/H_2SO_4 (piranha) solution to dissolve the junction materials without damaging the Au substrate, allowing microfabricated samples to be recycled and used many times, *viz.* Figure 8, for SEM images.

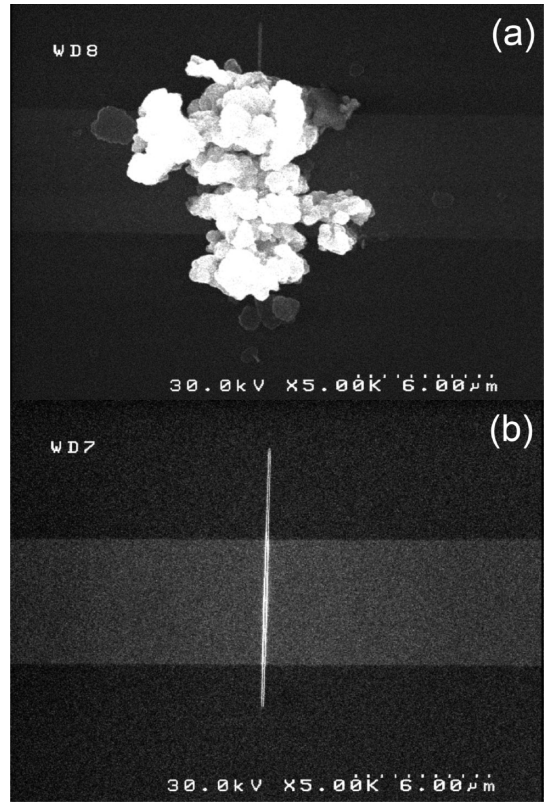

Figure 8. (a) SEM image of a heavily overgrown Au−Ag−Au bimetallic junction. (b) SEM image of the same sample after the overgrown Ag was removed by etching in piranha. The nanogap initial state was recovered without damage.

CONCLUSIONS

The work described here represents a fundamental advance over the use of open-WE electrochemistry to prepare monometallic ASJs. Using the open-WE protocol to achieve extremely slow electrochemical reaction rates greatly enhances the controllability of nanofabrication, allowing production of Au−Cu−Au and Au−Ag−Au bimetallic ASJs that show remarkable stability, exhibiting steady conductance values for over 3 h in favorable cases. Au−Cu−Au ASJs display more complicated behavior, highlighted by spontaneous restructuring dynamics at open circuit. These dynamics, if unchecked, always result in a zero conductance state on a time scale of a few minutes. However, if a sufficiently negative potential, E_{DC}, is applied, the Au−Cu−Au structures can be stabilized. The stable structures exist for periods of up to tens of minutes, over which time the slowed restructuring dynamics can produce a number of intermediate states, even fractional conductance states at long times. Stabilization of Au−Cu−Au ASJs could arise from two possible sources: hydrogen adsorption and potential-induced shift of the Fermi level. The stabilization of metal nanowires by adsorp-

tion of hydrogen has precedent in the literature, although the Fermi level shift cannot be discounted. The other striking feature of these results is the development of stable fractional conductance states for both Cu- and Ag-based bimetallic ASJs, which likely have their origin in physical restructuring.

Reproducible fabrication of bimetallic ASJs can be achieved by choosing metals such that the nanogap substrate (Au) is inert in the electroplating solution under the applied potentials needed to deposit or dissolve the second metal. Using this strategy, we were able to repeatedly and reproducibly fabricate Au−Ag−Au and Au−Cu−Au bimetallic ASJs both on open Si surfaces and in microfluidic channels. This capability opens the door to exciting applications of bimetallic ASJs, for example, as renewable detection elements in microfluidic devices for chemical and biochemical sensing.

EXPERIMENTAL SECTION

Template Fabrication. Fabrication of metallic ASJs employs three major steps. Beginning with a photolithographically defined Au microbridge, Au nanogaps are produced using focused ion beam (FIB) milling, then the ASJ is formed in a final electrochemical deposition/dissolution step employing selected metals in the nanogaps. The detailed procedure has been given previously.[34] Briefly, bowtie-shaped Au films (30 nm thick, 3 nm thick Cr as an adhesion layer) are formed on Si(100) covered with 500 nm of a thermal oxide (Silicon Quest International, CA) using standard photolithography and a lift-off process. A 5 μm wide × 100 μm long microbridge constitutes the center of each Au bowtie. A thin layer of SiN_x (~100 nm thick) is then deposited by plasma-enhanced chemical vapor deposition to protect the Au films. After exposing the contact pads by etching away the SiN_x layer on both sides of each sample, a narrow slot ($d \leq$ 100 nm) is opened in the SiN_x−Au−SiO_2 sandwich structure using FIB milling on an FEI Helios NanoLab 600 (FEI Strata DB235 in some early experiments) dual-beam system in the region of the microbridge to form a nanogap. These SiN_x-protected Au nanogaps are ideal for electrochemical fabrication of ASJs because only a narrow band of exposed metal exists in the nanogap.

ASJ Formation and Characterization. Metal ASJs are created in the nanogaps *via* electrodeposition for the nanogap samples or electrodissolution for the overgrown junctions by the open-WE protocol. All electrochemistry is carried out in 0.1 M K_2SO_4 containing 1 mM $CuSO_4$ (for Cu ASJs) or 1 mM Ag_2SO_4 (for Ag ASJs) as the electroplating solution at 300 K. All chemicals are from Fisher, ACS certified, and are used without further purification. The fabrication process is monitored *in situ* by measuring the AC voltage drop across an external load resistance (either 10 kΩ or 100 Ω depending on the conductance of the sample), connected in series with the sample. A small (typically 100 μV) AC excitation, V_{AC}, is placed across the nanogap, and the resulting AC current is measured using a lock-in amplifier (Stanford Research Systems, SR830). A schematic diagram of the experimental apparatus is shown in Figure 1a. In the case of ASJs fabricated directly on the surface, a removable Au wire (0.25 mm in diameter) serves as both the counter electrode (CE) and quasi-reference electrode (QRE), while for fabrication of ASJs in microfluidic channels, a 200 μm wide (same thickness as the microbridge) Au wire is patterned on the chip surface to serve as the CE/QRE. The fabrication process can be terminated at any time by either disconnecting CE/QRE or removing it from the solution (if it is removable). Physical removal of the CE/QRE frequently results in a brief current spike which is removed from the data for clarity. Microfluidic channels (typical width 400 μm) are fabricated by casting a mixture of polydimethylsiloxane (PDMS) prepolymer and curing agent (Sylgard 184, Dow Corning) on an SU-8 mold of the appropriate dimensions.[62] After curing overnight, the PDMS channel is carefully aligned to the center of the chip surface, exposing the Au microbridge area as well as a part of the CE/QRE in the channel. The electroplating solution is then slowly introduced into the microfluidic channel using a syringe pump for electrodeposition and dissolution (see Figure 1b,c). Scanning electron microscopy (SEM) measurements were carried out using a Hitachi 4500 SEM operating at 20 or 30 kV and an emission current of 20 μA.

Acknowledgment. This work was supported by the National Science Foundation through Grant NSF 0807816 and by the U.S. Army Corps of Engineers (W9132T-07-2-0003).

REFERENCES AND NOTES

1. Ohnishi, H.; Kondo, Y.; Takayanagi, K. Quantized Conductance through Individual Rows of Suspended Gold Atoms. *Nature* **1998**, *395*, 780–783.
2. Yanson, A. I.; Bollinger, G. R.; van den Brom, H. E.; Agrait, N.; van Ruitenbeek, J. M. Formation and Manipulation of a Metallic Wire of Single Gold Atoms. *Nature* **1998**, *395*, 783–785.
3. Agrait, N.; Yeyati, A. L.; van Ruitenbeek, J. M. Quantum Properties of Atomic-Sized Conductors. *Phys. Rep.* **2003**, *377*, 81–279.
4. Parks, J. J.; Champagne, A. R.; Hutchison, G. R.; Flores-Torres, S.; Abruna, H. D.; Ralph, D. C. Tuning the Kondo Effect with a Mechanically Controllable Break Junction. *Phys. Rev. Lett.* **2007**, *99*, 026601.
5. Pauly, F.; Dreher, M.; Viljas, J. K.; Hafer, M.; Cuevas, J. C.; Nielaba, P. Theoretical Analysis of the Conductance Histograms and Structural Properties of Ag, Pt, and Ni Nanocontacts. *Phys. Rev. B* **2006**, *74*, 235106.
6. Dreher, M.; Pauly, F.; Heurich, J.; Cuevas, J. C.; Scheer, E.; Nielaba, P. Structure and Conductance Histogram of Atomic-Sized Au Contacts. *Phys. Rev. B* **2005**, *72*, 075435.
7. Snow, E. S.; Park, D.; Campbell, P. M. Single-Atom Point Contact Devices Fabricated with an Atomic Force Microscope. *Appl. Phys. Lett.* **1996**, *69*, 269–271.
8. Rubio, G.; Agrait, N.; Vieira, S. Atomic-Sized Metallic Contacts: Mechanical Properties and Electronic Transport. *Phys. Rev. Lett.* **1996**, *76*, 2302–2305.
9. Kroger, J.; Neel, N.; Sperl, A.; Wang, Y. F.; Berndt, R. Single-Atom Contacts with a Scanning Tunnelling Microscope. *New J. Phys.* **2009**, *11*, 125006.
10. Krans, J. M.; Muller, C. J.; Yanson, I. K.; Govaert, T. C. M.; Hesper, R.; van Ruitenbeek, J. M. One-Atom Point Contacts. *Phys. Rev. B* **1993**, *48*, 14721–14724.
11. Limot, L.; Kroger, J.; Berndt, R.; Garcia-Lekue, A.; Hofer, W. A. Atom Transfer and Single-Adatom Contacts. *Phys. Rev. Lett.* **2005**, *94*, 126102.
12. Neel, N.; Kroger, J.; Limot, L.; Palotas, K.; Hofer, W. A.; Berndt, R. Conductance and Kondo Effect in a Controlled Single-Atom Contact. *Phys. Rev. Lett.* **2007**, *98*, 016801.
13. Untiedt, C.; Caturla, M. J.; Calvo, M. R.; Palacios, J. J.; Segers, R. C.; van Ruitenbeek, J. M. Formation of a Metallic Contact: Jump to Contact Revisited. *Phys. Rev. Lett.* **2007**, *98*, 206801.
14. Ittah, N.; Yutsis, I.; Selzer, Y. Fabrication of Highly Stable Configurable Metal Quantum Point Contacts. *Nano Lett.* **2008**, *8*, 3922–3927.
15. Park, J.; Pasupathy, A. N.; Goldsmith, J. I.; Chang, C.; Yaish, Y.; Petta, J. R.; Rinkoski, M.; Sethna, J. P.; Abruna, H. D.; McEuen, P. L.; Ralph, D. C. Coulomb Blockade and the Kondo Effect in Single-Atom Transistors. *Nature* **2002**, *417*, 722–725.

16. Calvo, M. R.; Fernandez-Rossier, J.; Palacios, J. J.; Jacob, D.; Natelson, D.; Untiedt, C. The Kondo Effect in Ferromagnetic Atomic Contacts. *Nature* **2009**, *458*, 1150–U85.
17. Xie, F. Q.; Maul, R.; Augenstein, A.; Obermair, C.; Starikov, E. B.; Schon, G.; Schimmel, T.; Wenzel, W. Independently Switchable Atomic Quantum Transistors by Reversible Contact Reconstruction. *Nano Lett.* **2008**, *8*, 4493–4497.
18. Xie, F. Q.; Nittler, L.; Obermair, C.; Schimmel, T. Gate-Controlled Atomic Quantum Switch. *Phys. Rev. Lett.* **2004**, *93*, 128303.
19. Li, C. Z.; He, H. X.; Bogozi, A.; Bunch, J. S.; Tao, N. J. Molecular Detection Based on Conductance Quantization of Nanowires. *Appl. Phys. Lett.* **2000**, *76*, 1333–1335.
20. Bogozi, A.; Lam, O.; He, H. X.; Li, C. Z.; Tao, N. J.; Nagahara, L. A.; Amlani, I.; Tsui, R. Molecular Adsorption onto Metallic Quantum Wires. *J. Am. Chem. Soc.* **2001**, *123*, 4585–4590.
21. Li, C. Z.; Sha, H.; Tao, N. J. Adsorbate Effect on Conductance Quantization in Metallic Nanowires. *Phys. Rev. B* **1998**, *58*, 6775–6778.
22. He, H. X.; Shu, C.; Li, C. Z.; Tao, N. J. Adsorbate Effect on the Mechanical Stability of Atomically Thin Metallic Wires. *J. Electroanal. Chem.* **2002**, *522*, 26–32.
23. Kiguchi, M.; Djukic, D.; van Ruitenbeek, J. M. The Effect of Bonding of a CO Molecule on the Conductance of Atomic Metal Wires. *Nanotechnology* **2007**, *18*, 035205.
24. Castle, P. J.; Bohn, P. W. Interfacial Scattering at Electrochemically Fabricated Atom-Scale Junctions between Thin Gold Film Electrodes in a Microfluidic Channel. *Anal. Chem.* **2005**, *77*, 243–249.
25. Landauer, R. Spatial Variation of Currents and Fields Due to Localized Scatterers in Metallic Conduction. *IBM J. Res. Dev.* **1957**, *1*, 223–231.
26. Olesen, L.; Laegsgaard, E.; Stensgaard, I.; Besenbacher, F.; Schiotz, J.; Stoltze, P.; Jacobsen, K. W.; Norskov, J. K. Quantized Conductance in an Atom-Sized Point-Contact. *Phys. Rev. Lett.* **1994**, *72*, 2251–2254.
27. van Ruitenbeek, J. M.; Alvarez, A.; Pineyro, I.; Grahmann, C.; Joyez, P.; Devoret, M. H.; Esteve, D.; Urbina, C. Adjustable Nanofabricated Atomic Size Contacts. *Rev. Sci. Instrum.* **1996**, *67*, 108–111.
28. Li, C. Z.; Tao, N. J. Quantum Transport in Metallic Nanowires Fabricated by Electrochemical Deposition/Dissolution. *Appl. Phys. Lett.* **1998**, *72*, 894–896.
29. He, H. X.; Boussaad, S.; Xu, B. Q.; Li, C. Z.; Tao, N. J. Electrochemical Fabrication of Atomically Thin Metallic Wires and Electrodes Separated with Molecular-Scale Gaps. *J. Electroanal. Chem.* **2002**, *522*, 167–172.
30. Meszaros, G.; Kronholz, S.; Karthauser, S.; Mayer, D.; Wandlowski, T. Electrochemical Fabrication and Characterization of Nanocontacts and nm-Sized Gaps. *Appl. Phys. A: Mater. Sci. Process.* **2007**, *87*, 569–575.
31. Li, J. Z.; Yamada, Y.; Murakoshi, K.; Nakato, Y. Sustainable Metal Nano-contacts Showing Quantized Conductance Prepared at a Gap of Thin Metal Wires in Solution. *Chem. Commun.* **2001**, 2170–2171.
32. Umeno, A.; Hirakawa, K. Fabrication of Atomic-Scale Gold Junctions by Electrochemical Plating Using a Common Medical Liquid. *Appl. Phys. Lett.* **2005**, *86*, 054103.
33. Calvo, M. R.; Mares, A. I.; Climent, V.; van Ruitenbeek, J. M.; Untiedt, C. Formation of Atomic-Sized Contacts Controlled by Electrochemical Methods. *Phys. Status Solidi A* **2007**, *204*, 1677–1685.
34. Shi, P.; Bohn, P. W. Stable Atom-Scale Junctions on Silicon Fabricated by Kinetically Controlled Electrochemical Deposition and Dissolution. *ACS Nano* **2008**, *2*, 1581–1588.
35. Li, C. Z.; Bogozi, A.; Huang, W.; Tao, N. J. Fabrication of Stable Metallic Nanowires with Quantized Conductance. *Nanotechnology* **1999**, *10*, 221–223.
36. Li, J. Z.; Kanzaki, T.; Murakoshi, K.; Nakato, Y. Metal-Dependent Conductance Quantization of Nanocontacts in Solution. *Appl. Phys. Lett.* **2002**, *81*, 123–125.
37. Qi, W. H.; Wang, M. P. Size Effect on the Cohesive Energy of Nanoparticle. *J. Mater. Sci. Lett.* **2002**, *21*, 1743–1745.
38. Kittel, C. *Introduction to Solid State Physics*; Wiley: New York, 2000.
39. Qi, W. H.; Wang, M. P.; Xu, G. Y. The Particle Size Dependence of Cohesive Energy of Metallic Nanoparticles. *Chem. Phys. Lett.* **2003**, *372*, 632–634.
40. Santos, E.; Quaino, P.; Soldano, G.; Schmickler, W. Electrochemical Reactivity and Fractional Conductance of Nanowires. *Electrochem. Commun.* **2009**, *11*, 1764–1767.
41. Nautiyal, T.; Youn, S. J.; Kim, K. S. Effect of Dimensionality on the Electronic Structure of Cu, Ag, and Au. *Phys. Rev. B* **2003**, *68*, 033407.
42. Xu, B. Q.; He, H. X.; Boussaad, S.; Tao, N. J. Electrochemical Properties of Atomic-Scale Metal Wires. *Electrochim. Acta* **2003**, *48*, 3085–3091.
43. Xu, B. Q.; He, H. X.; Tao, N. J. Controlling the Conductance of Atomically Thin Metal Wires with Electrochemical Potential. *J. Am. Chem. Soc.* **2002**, *124*, 13568–13575.
44. Shu, C.; Li, C. Z.; He, H. X.; Bogozi, A.; Bunch, J. S.; Tao, N. J. Fractional Conductance Quantization in Metallic Nanoconstrictions under Electrochemical Potential Control. *Phys. Rev. Lett.* **2000**, *84*, 5196–5199.
45. Kiguchi, M.; Konishi, T.; Miura, S.; Murakoshi, K. The Effect of Hydrogen Evolution Reaction on Conductance Quantization of Au, Ag, Cu Nanocontacts. *Nanotechnology* **2007**, *18*, 424011.
46. Kiguchi, M.; Konishi, T.; Hasegawa, K.; Shidara, S.; Murakoshi, K. Three Reversible States Controlled on a Gold Monoatomic Contact by the Electrochemical Potential. *Phys. Rev. B* **2008**, *77*, 245421.
47. Kiguchi, M.; Konishi, T.; Murakoshi, K. Conductance Bistability of Gold Nanowires at Room Temperature. *Phys. Rev. B* **2006**, *73*, 125406.
48. Li, J. Z.; Nakato, Y.; Murakoshi, K. Electrochemical Fabrication of Pd−Au Heterogeneous Nanocontact Showing Stable Conductance Quantization under Applying High Bias Voltage. *Chem. Lett.* **2005**, *34*, 374–375.
49. Csonka, S.; Halbritter, A.; Mihaly, G. Pulling Gold Nanowires with a Hydrogen Clamp: Strong Interactions of Hydrogen Molecules with Gold Nanojunctions. *Phys. Rev. B* **2006**, *73*, 075405.
50. Csonka, S.; Halbritter, A.; Mihaly, G.; Jurdik, E.; Shklyarevskii, O. I.; Speller, S.; van Kempen, H. Fractional Conductance in Hydrogen-Embedded Gold Nanowires. *Phys. Rev. Lett.* **2003**, *90*, 116803.
51. Hakkinen, H.; Barnett, R. N.; Landman, U. Gold Nanowires and Their Chemical Modifications. *J. Phys. Chem. B* **1999**, *103*, 8814–8816.
52. Barnett, R. N.; Hakkinen, H.; Scherbakov, A. G.; Landman, U. Hydrogen Welding and Hydrogen Switches in a Monatomic Gold Nanowire. *Nano Lett.* **2004**, *4*, 1845–1852.
53. Skorodumova, N. V.; Simak, S. I. Stability of Gold Nanowires at Large Au−Au Separations. *Phys. Rev. B* **2003**, *67*, 121404.
54. Kiguchi, M.; Konishi, T.; Murakoshi, K. Electrochemical Potential Control of Stretched Length of Au Nanowire in Solution. *Chem. Lett.* **2005**, *34*, 1336–1337.
55. Thijssen, W. H. A.; Marjenburgh, D.; Bremmer, R. H.; van Ruitenbeek, J. M. Oxygen-Enhanced Atomic Chain Formation. *Phys. Rev. Lett.* **2006**, *96*, 026806.
56. Kiguchi, M.; Murakoshi, K. Fabrication of Stable Pd Nanowire Assisted by Hydrogen in Solution. *Appl. Phys. Lett.* **2006**, *88*, 253112.
57. Konishi, T.; Kiguchi, M.; Murakoshi, K. Quantized Conductance Behavior of Pt Metal Nanoconstrictions under Electrochemical Potential Control. *Surf. Sci.* **2007**, *601*, 4122–4126.
58. Kiguchi, M.; Miura, S.; Murakoshi, K. Fabrication of Stable Metal Nanowire Showing Conductance Quantization in Solution. *Surf. Sci.* **2007**, *601*, 4127–4130.
59. Kiguchi, M.; Konishi, T.; Murakoshi, K. Hydrogen-Assisted Stabilization of Ni Nanowires in Solution. *Appl. Phys. Lett.* **2005**, *87*, 043104.
60. Kiguchi, M.; Konishi, T.; Miura, S.; Murakoshi, K. Mechanical Fabrication of Metal Nano-contacts Showing Conductance

Quantization under Electrochemical Potential Control. *Physica E* **2005**, *29*, 530–533.
61. Makk, P.; Csonka, S.; Halbritter, A. Effect of Hydrogen Molecules on the Electronic Transport through Atomic-Sized Metallic Junctions in the Superconducting State. *Phys. Rev. B* **2008**, *78*, 045414.
62. McDonald, J. C.; Duffy, D. C.; Anderson, J. R.; Chiu, D. T.; Wu, H. K.; Schueller, O. J. A.; Whitesides, G. M. Fabrication of Microfluidic Systems in Poly(dimethylsiloxane). *Electrophoresis* **2000**, *21*, 27–40.